

DISCONTINUOUS GALERKIN METHODS FOR THE RADIATIVE TRANSPORT EQUATION.

JEAN-LUC GUERMOND*, G. KANSCHAT†, AND J.-C. RAGUSA‡

Abstract. This notes presents some recent results regarding the approximation of the linear radiative transfer equation using discontinuous Galerkin methods. The locking effect occurring in the diffusion limit with the upwind numerical flux is investigated and a correction technique is proposed.

Key words. finite elements, discontinuous Galerkin, neutron transport, diffusion limit

AMS subject classifications. 65N35, 65N22, 65F05, 35J05

1. Introduction. The linear radiative transfer equation describes the processes by which particles (photons, neutrons, ...) interact with a background medium. Such processes play a crucial role in stellar atmospheres, nuclear reactor analysis, and shielding applications. The Discontinuous Galerkin (DG) finite element technique has been introduced by Reed and Hill [16] and Lesaint and Raviart [13] in the early 1970s to specifically solve this equation. It has been observed in the literature that the DG approximation with the upwind flux locks when the physical medium is optically thick. In this case the width of the medium is many mean free paths and the interaction processes are scattering-dominated. In the present paper we adopt the terminology of Babuška and Suri [3]: “*a numerical scheme for the approximation of a parameter-dependent problem is said to exhibit locking if the accuracy of the approximations deteriorates as the parameter tends to a limiting value. A robust numerical scheme for the problem is one that is essentially uniformly convergent for all values of the parameter.*” The objective of this paper is to review the influence of the definition of the numerical flux of the DG method when the medium is optically thick.

The paper is organized as follows. Section 2 introduces notation and recalls the S_N transport equation. Section 3 describes the discrete formulation which is obtained when applying a discontinuous Galerkin technique to the S_N equations. The origin of the locking phenomenon occurring when the DG method is equipped with the upwind flux is identified in §4. A modified nu-

*Department of Mathematics, Texas A&M University, College Station, TX 77843 (guermond@math.tamu.edu).

†Heidelberg University, Im Neuenheimer Feld 368 69120 Heidelberg, guido.kanschat@iwr.uni-heidelberg.de

‡Department of Nuclear Engineering, Texas A&M University, College Station, TX 77843 (ragusa@ne.tamu.edu).

merical flux is analyzed in §5. Numerical results illustrating the performance of the modified numerical flux are presented at the end of this section.

2. Formulation of the problem and S_N discretization. We recall in this section the transport equation and we provide some notations for angular discretization. To keep the discussion simple, we limit ourselves to the one-group discrete-ordinates equations; these equations model one-group neutron transport and grey radiative transfer.

2.1. The transport equation. Let \mathcal{D} be the spatial domain in \mathbb{R}^d (with $d = 1, 2, 3$), $\partial\mathcal{D}$ be the boundary of \mathcal{D} , \mathbf{n} be the outward unit normal vector on $\partial\mathcal{D}$, and S^2 be the unit sphere in \mathbb{R}^3 . The set of propagation directions \mathcal{S} is defined as S^2 for $d = 3$ and as the projection of S^2 onto \mathbb{R}^d when $d = 1, 2$. For instance \mathcal{S} is the unit disk if $d = 2$ and \mathcal{S} is the unit segment $[-1, +1]$ if $d = 1$. This convention, which is common in the radiation transport community, means that radiation is accounted for as a three-dimensional effect even in lower dimensional geometries. The transport of particles is then modeled by the linear Boltzmann equation:

$$(2.1a) \quad \mathbf{\Omega} \cdot \nabla \Psi(\mathbf{\Omega}, \mathbf{x}) + \sigma_t(\mathbf{x})\Psi(\mathbf{\Omega}, \mathbf{x}) - \sigma_s(\mathbf{x})\bar{\Psi}(\mathbf{x}) = q(\mathbf{x}), \quad \forall (\mathbf{\Omega}, \mathbf{x}) \in \mathcal{S} \times \mathcal{D},$$

where $\bar{\Psi} = \frac{1}{4\pi} \int_{\mathcal{S}} \Psi(\mathbf{\Omega}, \mathbf{x}) d\mathbf{\Omega}$ is the the scalar flux, and the boundary conditions are

$$(2.1b) \quad \Psi(\mathbf{\Omega}, \mathbf{x}) = \Psi^{\text{inc}}(\mathbf{\Omega}, \mathbf{x}), \quad \forall (\mathbf{\Omega}, \mathbf{x}) \in \mathcal{S} \times \partial\mathcal{D}, \quad \mathbf{\Omega} \cdot \mathbf{n}(\mathbf{x}) < 0.$$

where \mathbf{n} is the outward unit normal vector on $\partial\mathcal{D}$. For simplicity, we have assumed that the scattering and the extraneous sources are isotropic; this assumption does not affect the conclusions of the analysis. The dependent variable is the angular flux $\Psi(\mathbf{\Omega}, \mathbf{x})$, and the independent variables $(\mathbf{\Omega}, \mathbf{x})$ span $\mathcal{S} \times \mathcal{D}$. The given data are the extraneous source term $q(\mathbf{x})$, the incoming boundary radiation $\Psi^{\text{inc}}(\mathbf{\Omega}, \mathbf{x})$, the scattering cross section $\sigma_s(\mathbf{x})$, and the absorption cross section $\sigma_a(\mathbf{x}) := \sigma_t(\mathbf{x}) - \sigma_s(\mathbf{x})$.

2.2. The S_N discretization. A traditional way to approximate (2.1a) consists of dealing with \mathcal{S} and \mathcal{D} separately. In this paper the approximation with respect to the angles is done by using the so-called S_N -method. The S_N , or discrete-ordinates, version of (2.1a) is obtained by solving the transport equation along discrete directions (or ordinates) and by replacing the integrals over the unit sphere \mathcal{S} by quadratures. In the rest of the paper we assume that we have at hand a quadrature rule $\{(\mathbf{\Omega}_j, \omega_j), j = 1, \dots, n_\Omega\}$

$$(2.2) \quad \frac{1}{4\pi} \int_{\mathcal{S}} f(\mathbf{\Omega}, \mathbf{x}) d\mathbf{\Omega} \approx \sum_{j=1}^{n_\Omega} \omega_j f(\mathbf{\Omega}_j, \mathbf{x}),$$

satisfying the following properties:

$$(2.3) \quad \sum_{j=1}^{n_\Omega} \omega_j = 1, \quad \sum_{j=1}^{n_\Omega} \omega_j \boldsymbol{\Omega}_j = \mathbf{0},$$

$$(2.4) \quad \forall \mathbf{a}, \mathbf{b} \in \mathbb{R}^3, \quad \sum_{j=1}^{n_\Omega} \omega_j (\boldsymbol{\Omega}_j \cdot \mathbf{a})(\boldsymbol{\Omega}_j \cdot \mathbf{b}) = \frac{1}{3} \mathbf{a} \cdot \mathbf{b},$$

$$(2.5) \quad \exists c_0 > 0, \forall n_\Omega, \quad c_{\mathbf{n}} := \sum_{\boldsymbol{\Omega}_j \cdot \mathbf{n} < 0} \omega_j |\boldsymbol{\Omega}_j \cdot \mathbf{n}| \geq c_0.$$

Although it is a standard result that $\frac{1}{4\pi} \int_{\boldsymbol{\Omega} \cdot \mathbf{n} < 0} |\boldsymbol{\Omega} \cdot \mathbf{n}| \, d\boldsymbol{\Omega} = \frac{1}{4}$ for any unit vector \mathbf{n} , this equality may not exactly hold for any numerical quadrature at hand. However, reasonable sets of quadrature rules are such that this limit value is approached as the number of directions in the quadrature increases ($\lim_{n_\Omega \rightarrow \infty} c_{\mathbf{n}} = \frac{1}{4}$). In any case the hypothesis (2.5) holds whenever one can find d linearly independent vectors among the quadrature points $\boldsymbol{\Omega}_j$.

The S_N method consists of replacing the angular flux $\Psi(\boldsymbol{\Omega}, \mathbf{x})$ by a discrete angular flux $\psi(\mathbf{x}) = (\psi_1(\mathbf{x}), \psi_2(\mathbf{x}), \dots, \psi_{n_\Omega}(\mathbf{x}))$, and to convert the integro-differential equation (2.1) over $\mathcal{S} \times \mathcal{D}$ into a system of n_Ω coupled partial differential equations over \mathcal{D} for all the directions j as follows :

$$(2.6a) \quad \boldsymbol{\Omega}_j \cdot \nabla \psi_j(\mathbf{x}) + \sigma_t(\mathbf{x}) \psi_j(\mathbf{x}) - \sigma_s(\mathbf{x}) \bar{\psi}(\mathbf{x}) = q(\mathbf{x}), \quad \text{in } \mathcal{D},$$

with the inflow boundary condition

$$(2.6b) \quad \psi_j(\mathbf{x}) = \Psi_j^{\text{inc}}(\mathbf{x}), \quad \forall \mathbf{x} \in \partial\mathcal{D} \text{ with } \boldsymbol{\Omega}_j \cdot \mathbf{n}(\mathbf{x}) < 0.$$

The discrete scalar flux is defined by:

$$(2.7) \quad \bar{\psi}(\mathbf{x}) = \sum_{j=1}^{n_\Omega} \omega_j \psi_j(\mathbf{x}).$$

The discrete angular flux ψ is said to be isotropic when $\psi_j = \bar{\psi}$, for all $j \in \{1, \dots, n_\Omega\}$. In order to simplify the notation in subsequent sections, we introduce the discrete current vector $\mathbf{J}(\psi)$, also known as the first angular moment of ψ , as follows:

$$(2.8) \quad \mathbf{J}(\psi) = \sum_{j=1}^{n_\Omega} \omega_j \psi_j(\mathbf{x}) \boldsymbol{\Omega}_j.$$

Note that $\mathbf{J}(\psi) = \mathbf{0}$ whenever ψ is isotropic.

2.3. Diffusion limit. We say that the medium is optically thick when it takes many mean free paths for particles to cross the domain. In order to better understand the behavior of the solutions of the linear Boltzmann equation in this regime, we rescale the equation under the assumption that the ratio between the mean free path between two scattering events and the characteristic size (diameter) of the domain goes to zero. A measure of this ratio is given by

$$(2.9) \quad \varepsilon = \frac{1}{\sigma_s \text{diam}(\mathcal{D})}.$$

This parameter is well known to characterize the diffusivity of the problem, see for instance Larsen et al. [12] and Dautray and Lions [5, Chapter XXI]. We assume throughout this section that σ_s is constant over the domain to simplify the analysis. Then, we assume the following behaviors

$$(2.10) \quad \sigma_s = \varepsilon^{-1} \tilde{\sigma}_s, \quad \sigma_a = \varepsilon \tilde{\sigma}_a, \quad q = \varepsilon \tilde{q},$$

where the tilde quantities are independent of ε (note in particular that $\tilde{\sigma}_s = 1/\text{diam}(\mathcal{D})$). As ε goes to zero, the scattering and total cross sections take large values and the absorption cross section becomes small, rendering the configuration optically thick and diffusive.

Using (2.10), the scaled version of the transport equation (2.1) becomes

$$(2.11) \quad \boldsymbol{\Omega} \cdot \nabla \Psi(\boldsymbol{\Omega}, \mathbf{x}) + \left(\frac{\tilde{\sigma}_s}{\varepsilon} + \varepsilon \tilde{\sigma}_a \right) \Psi(\boldsymbol{\Omega}, \mathbf{x}) - \frac{\tilde{\sigma}_s}{\varepsilon} \bar{\Psi}(\mathbf{x}) = \varepsilon \tilde{q}(\mathbf{x}).$$

It is now well understood (see e.g., Chandrasekhar [4], Larsen et al. [12], and Dautray and Lions [5, Chapter XXI]) that $\lim_{\varepsilon \rightarrow 0} \Psi(\boldsymbol{\Omega}, \mathbf{x}) = \lim_{\varepsilon \rightarrow 0} \bar{\Psi}(\mathbf{x}) = \varphi(\mathbf{x})$, where the scalar flux φ satisfies the diffusion problem

$$(2.12a) \quad -\nabla \cdot \left(\frac{1}{3\tilde{\sigma}_s} \nabla \varphi \right) + \tilde{\sigma}_a \varphi = \tilde{q},$$

$$(2.12b) \quad \varphi(\mathbf{x}) = \frac{1}{2\pi} \int_{\boldsymbol{\Omega} \cdot \mathbf{n}(\mathbf{x}) < 0} W(|\boldsymbol{\Omega} \cdot \mathbf{n}(\mathbf{x})|) \Psi^{\text{inc}}(\boldsymbol{\Omega}, \mathbf{x}) \, d\boldsymbol{\Omega}, \quad \forall \mathbf{x} \in \partial D,$$

where $W(\mu) = \frac{\sqrt{3}}{2} \mu H(\mu)$ is defined in terms of Chandrasekhar's H -function for isotropic scattering in a conservative medium (see Malvagi and Pomraning [14] for the asymptotic analysis and Chandrasekhar [4] for details on the H -function). It is shown in Malvagi and Pomraning [14] that $\lim_{\varepsilon \rightarrow 0} \Psi = \varphi$, and the convergence is not uniform unless the incident flux is isotropic.

It is remarkable that under the assumptions made for the angular quadrature, the diffusion limit of the solution to the semi-discrete problem (2.6) (discrete-ordinate transport equation) has the same limit properties, i.e.,

$$(2.13) \quad \lim_{\varepsilon \rightarrow 0} \psi_j(\mathbf{x}) = \lim_{\varepsilon \rightarrow 0} \bar{\psi}(\mathbf{x}) = \varphi(\mathbf{x}), \quad \forall j \in \{1, \dots, n_\Omega\}.$$

The goal of the present paper is to determine when the above property holds when space is approximated using Discontinuous Galerkin methods.

3. DG Discretization. We now proceed with the spatial discretization of the S_N transport equation using DG finite elements.

3.1. The mesh. Let \mathbb{T}_h be a subdivision of \mathcal{D} into disjoint (open) cells K such that the closure of \mathcal{D} is equal to $\cup_{K \in \mathbb{T}_h} \overline{K}$. The meshes are assumed to be affine to avoid unnecessary technicalities; i.e., \mathcal{D} is assumed to be a polyhedron. The diameter of $K \in \mathbb{T}_h$ is denoted by h_K , and we set $h = \max_{K \in \mathbb{T}_h} h_K$. We suppose that we have at hand a family of meshes $\{\mathbb{T}_h\}$ and that this family is uniformly shape-regular. We also assume that the mesh is quasi-uniform; i.e., there is $c > 0$ so that

$$(3.1) \quad ch \leq h_K \leq h \quad \forall K \in \mathbb{T}_h.$$

This hypothesis is used when invoking inverse inequalities. It could be avoided by localizing the inverse estimate arguments, but we shall refrain from doing so to steer clear of unnecessary technicalities.

We denote \mathbb{F}_h^i the set of interior faces (also called interfaces); each face $F \in \mathbb{F}_h^i$ is the intersection of the boundaries of two mesh cells. We assign a normal vector \mathbf{n} for each face $F \in \mathbb{F}_h^i$. While the choice of the normal vector is arbitrary for interior faces, all the weak formulations considered below are independent of this choice and thus well-defined. The set of faces on the domain boundary, $\partial\mathcal{D}$, is denoted \mathbb{F}_h^b . The set of interfaces and boundary faces is denoted $\mathbb{F}_h = \mathbb{F}_h^i \cup \mathbb{F}_h^b$.

3.2. The Discontinuous Galerkin (DG) setting. We define a discontinuous approximation space for the scalar flux based on the mesh \mathbb{T}_h as follows:

$$(3.2) \quad V_h = \{v \in L^2(\mathcal{D}) \mid \forall K \in \mathbb{T}_h, v|_K \in P_K, \},$$

where, denoting \mathbb{P}_k the set of polynomials of degree at most k , the finite-dimensional space P_K is assumed to contain \mathbb{P}_k , i.e.,

$$(3.3) \quad \mathbb{P}_k \subset P_K, \quad \forall K \in \mathbb{T}_h.$$

The discrete space for the angular flux, W_h , simply consists of copies of V_h for each of the discrete ordinates:

$$(3.4) \quad W_h = (V_h)^{n_\Omega}.$$

We finally introduce the spaces with zero boundary conditions

$$(3.5) \quad V_{0,h} = \{v \in V_h \mid v|_{\partial\mathcal{D}} = 0\}, \quad W_{0,h} = (V_{0,h})^{n_\Omega}.$$

3.3. The DG weak formulation. The DG formulation of the problem (2.6) consists of seeking $\psi \in W_h$ so that the following holds for all cells $K \in$

\mathbb{T}_h , for all test functions $v_j \in V_h$ supported on K , and for all direction $j \in \{1, \dots, n_\Omega\}$:

$$(3.6) \quad \int_K (-\psi_j \boldsymbol{\Omega}_j \cdot \nabla v_j + (\sigma_s + \sigma_a) \psi_j v_j - \sigma_s \bar{\psi} v_j) \, d\mathbf{x} \\ + \int_{\partial K} \widehat{\mathbf{F}}_j(\mathbf{x}) \cdot \mathbf{n} v_j \, d\mathbf{x} = \int_K q v_j \, d\mathbf{x}.$$

where the numerical flux¹ $\widehat{\mathbf{F}}_j$ has yet to be defined. The purpose of the numerical flux $\widehat{\mathbf{F}}_j(\mathbf{x}) \cdot \mathbf{n}$ is to approximate the quantity $\psi_j \boldsymbol{\Omega}_j \cdot \mathbf{n}$ at the mesh interfaces since this quantity is double-valued due to the discontinuous nature of the approximation. The above system is obtained by (i) multiplying the S_N equations for direction j with test function v_j , (ii) integrating the results by parts, and (iii) replacing the two-valued function $\psi_j \boldsymbol{\Omega}_j \cdot \mathbf{n}$ by the numerical flux $\widehat{\mathbf{F}}_j \cdot \mathbf{n}$.

3.4. Jumps and averages. Due to the discontinuous nature of the spatial approximation, functions $v \in V_h$ are double-valued on interior faces. Let $F \in \mathbb{F}_h^i$ be an interior face separating two mesh cells, K_1 and K_2 . The mean value and jump of a function $v \in V_h$ across F are defined as follows:

$$(3.7) \quad \{v\} = \frac{1}{2}(v_1 + v_2), \quad \llbracket v \rrbracket = v_1 - v_2,$$

where $v_1 := v|_{K_1}$ and $v_2 := v|_{K_2}$ are the restrictions of v on the mesh cells K_1 and K_2 , respectively. Obviously, $\{v\}$ does not depend on the numbering of the cells K_1 and K_2 , but the jump does (there is a sign change when exchanging the cells K_1 and K_2). However, since the weak bilinear forms (to be defined further below) contain the product of two jumps, the orientation of the unit normal vector does not matter. Let \mathbf{n}_1 and \mathbf{n}_2 be the unit normal vectors on F pointing towards K_2 and K_1 , respectively. The mean value of quantities containing a normal vector is actually a jump since

$$\{\mathbf{v}\mathbf{n}\} = \frac{1}{2}(v_1 \mathbf{n}_1 + v_2 \mathbf{n}_2) = \frac{1}{2}(v_1 - v_2) \mathbf{n}_1 = \frac{1}{2}(v_2 - v_1) \mathbf{n}_2.$$

For any v in V_h and any interior face $F \in \mathbb{F}_h^i$, we introduce the so-called upwind and downwind values of v at $\mathbf{x} \in F$, $v^\uparrow(\mathbf{x})$ and $v^\downarrow(\mathbf{x})$, respectively, as follows:

$$(3.8) \quad v^\uparrow(\mathbf{x}) = \begin{cases} v_1(\mathbf{x}), & \text{if } \boldsymbol{\Omega} \cdot \mathbf{n}_1(\mathbf{x}) \geq 0 \\ v_2(\mathbf{x}), & \text{if } \boldsymbol{\Omega} \cdot \mathbf{n}_1(\mathbf{x}) < 0. \end{cases} \quad v^\downarrow(\mathbf{x}) = \begin{cases} v_2(\mathbf{x}) & \text{if } \boldsymbol{\Omega} \cdot \mathbf{n}_1(\mathbf{x}) \geq 0 \\ v_1(\mathbf{x}) & \text{if } \boldsymbol{\Omega} \cdot \mathbf{n}_1(\mathbf{x}) < 0. \end{cases}$$

¹The term ‘‘flux’’ is used in two different contexts. In the radiation transport context, we use the terms ‘‘angular flux’’ and ‘‘scalar flux’’. In the DG context, we use the notion of ‘‘numerical flux’’. These two notions are unfortunately unrelated but commonly employed in the radiation transport and DG literature, respectively. To avoid confusion, we always try to use the proper adjective in this paper.

Observing that the following holds for any positive number ($\gamma \geq 0$):

$$(3.9) \quad \boldsymbol{\Omega} \cdot \mathbf{n}_1 \{v\} + \frac{1}{2} \gamma |\boldsymbol{\Omega} \cdot \mathbf{n}_1| \llbracket v \rrbracket = \boldsymbol{\Omega} \cdot \mathbf{n}_1 \left(v^\uparrow(\mathbf{x}) + \frac{1}{2}(\gamma - 1)(v^\uparrow(\mathbf{x}) - v^\downarrow(\mathbf{x})) \right),$$

we obtain that

$$(3.10) \quad \boldsymbol{\Omega} \cdot \mathbf{n}_1 \{v\} + \frac{\gamma}{2} |\boldsymbol{\Omega} \cdot \mathbf{n}_1| \llbracket v \rrbracket = \begin{cases} \boldsymbol{\Omega} \cdot \mathbf{n}_1 v^\uparrow(\mathbf{x}) & \text{if } \gamma = 1, \\ \boldsymbol{\Omega} \cdot \mathbf{n}_1 \{v\} & \text{if } \gamma = 0. \end{cases}$$

The so-called upwind DG numerical flux is obtained with (3.9) by using $\gamma = 1$, and the centered numerical flux is obtained by using $\gamma = 0$. The representation (3.9) gives an easy way to construct numerical fluxes by modifying the coefficient γ .

4. The upwind approximation. In the radiative transfer literature it is common to replace $\widehat{\mathbf{F}}_j(\mathbf{x})$ in (3.6) by the upwind flux

$$(4.1) \quad \widehat{\mathbf{F}}_j \cdot \mathbf{n} = \boldsymbol{\Omega}_j \cdot \mathbf{n} \psi_j^\uparrow(\mathbf{x}).$$

We focus in this section on the consequences of this choice. We show in particular that it leads to locking in the diffusive regime for some families of approximation spaces.

4.1. Locking in the diffusion regime. It has been observed in the literature that the DG approximation (3.6) equipped with the upwind flux locks when the medium is optically thick. For instance, it is pointed out in Larsen [9, 8] that the so-called “step scheme”, a finite volume scheme (i.e., a piecewise constant DG scheme) with standard upwind, locks in the diffusion limit. A modification of the “step scheme” depending upon the total mean free path was proposed in Larsen [8] to correct the locking of the method in the diffusion limit, but this required modifying the streaming term and abandoning particle balance. Several other variations of the “step scheme” have been analyzed in Larsen et al. [12]: it was shown that the “Lund-Wilson” and the “Castor” variants of the step scheme yielded cell-edge angular fluxes that lock in the diffusion limit, and that the auxiliary relations linking the outgoing edge angular flux to the cell-average angular flux employ a multiplicative factor that depends on the mesh cell optical thickness in the direction traveled. Furthermore, the cell-edge fluxes for these schemes can not reproduce the infinite medium solution. A “new” scheme was proposed in Larsen et al. [12] but was subsequently dismissed due its a poor behavior at the boundaries. For many years, the diamond-difference scheme was found to be the best performing finite-difference scheme, even though its cell-edge fluxes lock in the thick diffusion limit. In Larsen and Morel [11], most of the previous schemes have been set aside in favor of the Linear Discontinuous finite element scheme (the piecewise linear DG technique with standard upwinding).

Adams [1] analyzed multi-dimensional DG approximations and showed that some schemes lock in the diffusion limit because the upwind method forces the scalar flux, and thus the angular flux, to be continuous across mesh cells. This observation is essential to understand what happens.

4.2. Convergence analysis. In the rest of the paper we adopt the scaling defined in (2.10) and consider the rescaled transport equation (2.11).

The observations and analysis of Adams [1] have been confirmed in Guermond and Kanschat [7], where the equivalence of the limit problem to a mixed discretization for the Laplacian was proved and the nature of the boundary layers was discussed. To better formulate the conclusions from Guermond and Kanschat [7], we introduce the subspace of V_h composed of the functions that are continuous:

$$(4.2) \quad C_h = V_h \cap C^0(\overline{\mathcal{D}}),$$

and we define $m(\mathbf{x}) := \frac{1}{\pi} \int_{\Omega \cdot \mathbf{n}(\mathbf{x}) < 0} \Psi^{\text{inc}}(\Omega, \mathbf{x}) |\Omega \cdot \mathbf{n}(\mathbf{x})| d\Omega$. The first key result is the following:

LEMMA 4.1. *Assume that m is the trace of a function in C_h . Then the solution of (3.6) with the upwind flux (4.1) is such that*

$$(4.3) \quad \lim_{\varepsilon \rightarrow 0} \psi_j \in C_h, \quad \forall j \in \{0, \dots, n_\Omega\}.$$

Remark 4.1. An immediate consequence of this result is that while piecewise constant approximation is admissible for solving the transport problem (2.1a) (or (2.11)), the continuity condition (4.3) forces the diffusion limit solution to be globally constant. This leads to locking, i.e., $\lim_{\varepsilon \rightarrow 0} \psi_j$ does not converge to φ when using DG0 with the upwind flux, unless φ is constant.

Let us further assume that the following approximation properties hold:

$$(4.4) \quad \inf_{v_h \in \mathcal{C}_{h,0}} \|\phi - v_h\|_{H^p(D)} \leq ch^{l-p} \|\phi\|_{H^l(D)}, \quad \forall \phi \in H^l(D), \forall p \in [0, 1], \forall l \in [1, 2],$$

$$(4.5) \quad \inf_{v_h \in \mathcal{C}_{h,0}} (\|\phi - v_h\|_{L^2(\partial D)} + h \|\partial_n(\phi - v_h)\|_{L^2(\partial D)}) \leq ch^{l-\frac{1}{2}} \|\phi\|_{H^l(D)} \quad \forall l \in [1, 2].$$

The following result is then proved in Guermond and Kanschat [7]:

THEOREM 4.2. *Assume that Ψ^{inc} is isotropic and smooth enough and that (4.4)–(4.5) hold. Then the solution of (3.6) with the upwind flux (4.1) converges in $H^1(\mathcal{D})$ to φ , solution of (2.12a)–(2.12b), and the following error estimate holds:*

$$(4.6) \quad \|\lim_{\varepsilon \rightarrow 0} \psi_j - \varphi\|_{H^1(\mathcal{D})} \leq c \inf_{v_h \in \mathcal{C}_{h,0}} \|\varphi - v_h\|_{H^1(\mathcal{D})}, \quad \forall j \in \{0, \dots, n_\Omega\}.$$

The critical assumption here is (4.4), which requires the spaces C_h to be rich enough so as to have reasonable approximation properties. This is a condition on the mesh family $\{\mathbb{T}_h\}_{h>0}$ and the associated discrete space family $\{V_h\}_{h>0}$. More precisely (4.4) holds if the following two conditions are satisfied:

(i) The meshes are conforming; i.e., each face of a cell is either the face of a neighboring cell or at the boundary. This condition can be weakened to accommodate for local refinement, and in this case each face of any cell may be a subset of a face of its neighbor.

(ii) The polynomial spaces on each cell must allow continuity across interfaces of neighboring cells without losing approximation properties. This is usually achieved by using multidimensional polynomial spaces \mathbb{P}_k of total order $k \geq 1$ for triangles and tetrahedra or mapped tensor product spaces \mathbb{Q}_k of order $k \geq 1$ in each coordinate direction on quadrilaterals and hexahedra.

Remark 4.2. For instance, condition (ii) is violated if piecewise constant elements are used.

Remark 4.3. Conditions (i)–(ii) have been identified in Adams [1] and termed “locality” and “surface-matching” properties. We think though that the condition (4.4) gives a complementary rationale to that given in Adams [1]. Lists of admissible and nonadmissible finite elements are given in Tables I and II in Adams [1].

When the incoming flux at the boundary is not isotropic some boundary layer effect occur as mentioned in Adams [1] and Larsen and Keller [10]. To formulate a precise result we introduce the function $\mathbf{M}(\mathbf{x}) := \frac{1}{4\pi} \int_{\Omega \cdot \mathbf{n}(\mathbf{x}) < 0} \Psi^{\text{inc}}(\Omega, \mathbf{x}) |\Omega \cdot \mathbf{n}(\mathbf{x})| \Omega \, d\Omega$.

THEOREM 4.3. *Assume that $\mathbf{M}(\mathbf{x}) \cdot \mathbf{n}$ is the trace of a function in C_h and (4.4)–(4.5) hold. Then the solution of (3.6) with the upwind flux (4.1) converges to a limit ψ_{lim} in $H^s(\mathcal{D})$ for all $s \in [0, \frac{1}{2})$ and*

$$(4.7) \quad \left\| \lim_{\varepsilon \rightarrow 0} \psi_j - \psi_{\text{lim}} \right\|_{L^2(\mathcal{D})} \leq c h^{\frac{s}{3}}, \quad \forall s \in [0, \frac{1}{2}), \quad \forall j \in \{0, \dots, n_\Omega\}$$

That the above convergence occurs in a space $H^s(\mathcal{D})$ with $s < \frac{1}{2}$ is the signature of boundary layer effects developing at the boundary when the incoming flux is not isotropic.

5. Robust DG approximation. The asymptotic analysis in Adams [1] and Guermond and Kanschat [7] suggests that the problem could be alleviated by modifying the upwind numerical flux. As pointed out in Ayuso and Marini [2], Ern and Guermond [6], the upwind numerical flux is only one particular choice among many for stabilization. By making the amount of stabilization dependent on the scattering cross section so that the amount of upwinding decreases as the scattering cross section increases, it is shown in Ragusa et al. [15] that locking can indeed be avoided in the thick diffusive limit.

5.1. Modified numerical flux. The new numerical flux proposed by Ragusa et al. [15] is based on (3.9). Before giving its expression we define the

following stabilization parameters

$$(5.1) \quad \gamma(\mathbf{x}) = \frac{\gamma_0}{\max(\gamma_0, \sigma_s(\mathbf{x}) \text{diam } \mathcal{D})}, \quad \delta(\mathbf{x}) = \delta_0 \frac{1 - \gamma(\mathbf{x})}{\gamma(\mathbf{x})},$$

where the parameters $\gamma_0 > 0$, $\delta_0 > 0$ are assumed to be of order one. The rationale for these definitions is as follows: γ tends to 0 in the diffusive limit, whereas γ converges 1 in the optically thin regions.

The following definition for the numerical flux across the interface $F \in \mathbb{F}_h^i$ from K_1 to K_2 is proposed in Ragusa et al. [15]:

$$(5.2) \quad \widehat{\mathbf{F}}_j(\mathbf{x}) \cdot \mathbf{n}_1 = \boldsymbol{\Omega}_j \cdot \mathbf{n}_1 \{\{\psi_j\}\} + \frac{\gamma(\mathbf{x})}{2} |\boldsymbol{\Omega}_j \cdot \mathbf{n}_1| [\![\psi_j]\!] + \frac{\delta(\mathbf{x})}{2} \{\{\mathbf{J}(\psi) \cdot \mathbf{n}\}\} \boldsymbol{\Omega}_j \cdot \mathbf{n}_1.$$

We use the standard upwind definition of the numerical flux for any boundary face $F \in F_h^b$:

$$(5.3) \quad \widehat{\mathbf{F}}_j(\mathbf{x}) \cdot \mathbf{n} = \begin{cases} \boldsymbol{\Omega}_j \cdot \mathbf{n} \Psi_j^{\text{inc}} & \text{if } \boldsymbol{\Omega}_j \cdot \mathbf{n}(\mathbf{x}) < 0 \\ \boldsymbol{\Omega}_j \cdot \mathbf{n} \psi_j & \text{otherwise.} \end{cases}$$

Note that the definition of $\gamma(\mathbf{x})$ is such that, on the one hand, $\gamma \rightarrow 0$ when the ratio of the scattering mean free path to the diameter of the domain is small (i.e., $\sigma_s(\mathbf{x})\mathcal{D}$ is large); on the other hand, γ is bounded away from zero when the mean free path is a non-negligible fraction of the diameter of the domain (the γ_0 constant assures that $\gamma(\mathbf{x}) \rightarrow 1$ when $\sigma_s(\mathbf{x})\mathcal{D}$ is small. The parameter δ is designed so that it goes to zero when $\gamma \rightarrow 1$ and behaves like $1/\gamma$ when $\gamma \rightarrow 0$. This behavior is dictated from the forthcoming asymptotic analysis. The intuitive motivations for the first and second terms in (5.2) are the expressions (3.9) and (3.10). The standard upwind numerical flux is obtained by setting $\gamma = 1$, which also implies $\delta = 0$. The justification for the third term $\{\{\mathbf{J}(\psi) \cdot \mathbf{n}\}\} \boldsymbol{\Omega}_j \cdot \mathbf{n}_1$ comes from the asymptotic analysis; this term turns out to be necessary for the limit problem to be well-posed.

5.2. Convergence analysis. In the rest of this section we assume that $\Psi^{\text{inc}} = 0$ and we refer the reader to Guermond and Kanschat [7] for the handling of inhomogeneous Dirichlet boundary conditions. The main result from Ragusa et al. [15] is the following:

PROPOSITION 1. *Let $\psi \in W_h$ be the solution to the S_N -DG problem (3.6) equipped with the numerical flux (5.2). Then ψ converges to an isotropic function $\varphi \in V_{0,h}$ as $\varepsilon \rightarrow 0$. Furthermore, there is a vector field $\mathbf{J} \in (V_h)^d$ so that the pair (φ, \mathbf{J}) solves the following DG system for all $v \in V_{0,h}$ and all*

$\mathbf{L} \in (V_h)^d$:

$$\begin{aligned}
 & \sum_{K \in \mathbb{T}_h} \int_K (\nabla \cdot \mathbf{J} + \tilde{\sigma}_a \varphi) v \, d\mathbf{x} \\
 & \quad + \sum_{F \in \mathbb{F}_h^i} \int_F \left(c_{\mathbf{n}_F} \frac{\gamma_0}{2} \llbracket \varphi \rrbracket \llbracket v \rrbracket - 2 \{ \{ \mathbf{J} \cdot \mathbf{n} \} \} \{ \{ v \} \} \right) d\mathbf{x} = \int_{\mathcal{D}} \tilde{q} v \, d\mathbf{x}, \\
 (5.4) \quad & \sum_{K \in \mathbb{T}_h} \int_K \left(\frac{1}{3} \nabla \varphi + \tilde{\sigma}_s \mathbf{J} \right) \cdot \mathbf{L} \, d\mathbf{x} \\
 & \quad + \sum_{F \in \mathbb{F}_h^i} \int_F \left(-\frac{2}{3} \{ \{ \varphi \mathbf{n} \} \} \{ \{ \mathbf{L} \} \} + \frac{\delta_0}{3\gamma_0} \{ \{ \mathbf{J} \cdot \mathbf{n} \} \} \{ \{ \mathbf{L} \cdot \mathbf{n} \} \} \right) d\mathbf{x} = 0,
 \end{aligned}$$

where $c_{\mathbf{n}_F} := \sum_{\Omega_j \cdot \mathbf{n}_F \leq 0} \omega_j |\Omega_j \cdot \mathbf{n}_F|$ is bounded away from zero uniformly with respect to $F \in \mathbb{F}_h^i$, h , and n_Ω .

The above result may seem obscure, but the limit problem (5.4) coincides exactly with the method from Ern and Guermond [6] (see §5.3 therein) that has been proposed to solve the limit problem (2.12a)–(2.12b) in mixed form:

$$(5.5a) \quad \nabla \cdot \mathbf{J} + \tilde{\sigma}_a \varphi = \tilde{q}$$

$$(5.5b) \quad \frac{1}{3} \nabla \varphi + \tilde{\sigma}_s \mathbf{J} = 0$$

$$(5.5c) \quad \varphi|_{\partial \mathcal{D}} = 0.$$

The theoretical convergence analysis from Ern and Guermond [6] implies that (5.4) is a consistent and convergent approximation of (2.12a)–(2.12b). That is, the discrete transport formulation (3.6) with the numerical flux (5.2) is robust and yields a convergent approximation of the diffusion equation as ε goes to zero.

5.3. Numerical Experiments. We finish this paper by numerically illustrating the above method. We solve the problem of local energy equilibrium in the domain $D = (-1, 1)^2 \times \mathbb{R}$ with zero incoming flux,

$$\Omega \cdot \nabla \psi(\Omega, x) + \frac{1}{\varepsilon} (\psi(\Omega, x) - \bar{\psi}(x)) = \frac{\varepsilon}{3} \frac{\pi^2}{4} \prod_{i=1}^2 \cos\left(\frac{\pi x_i}{2}\right).$$

The solution is independent of x_3 . We study the limit of DG approximations using the upwind flux (4.1) and the modified flux (5.2) as $\varepsilon \rightarrow 0$. The solution to the diffusion limit is $\varphi(\mathbf{x}) = \prod_{i=1}^d \cos\left(\frac{\pi x_i}{2}\right)$.

We use piecewise linear polynomials in space, and we choose γ and δ as in (5.1) with $\gamma_0 = 4$ and $\delta_0 = 1$. The results computed on a quadrangular mesh composed of 64 cells are shown in Figure 5.1 for $\varepsilon = 1, 2^{-6}, 2^{-10}$, and 2^{-14} . We observe that the solution obtained with the upwind flux locks when $\varepsilon \rightarrow 0$, whereas the solution computed with the modified flux converges to the correct diffusion limit as expected.

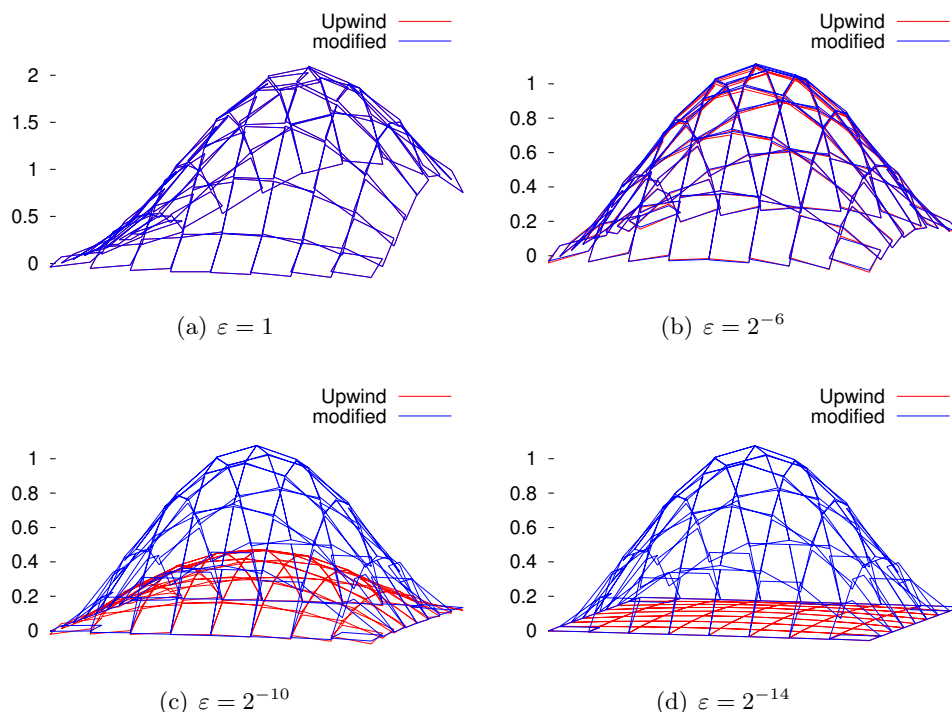


FIG. 5.1. Comparison of the solutions with upwind and modified flux with quadrangular \mathbb{P}_1 finite elements, respectively. As the scattering cross section increases, the upwind flux solution locks, while the other converges to the correct diffusion limit.

Acknowledgement. This material is based upon work supported by the Department of Homeland Security under agreement 2008-DN-077-ARI018-02, National Science Foundation grants DMS-0713829, DMS-0810387, and CBET-0736202, and is partially supported by award KUS-C1-016-04, made by King Abdullah University of Science and Technology (KAUST).

References.

- [1] M. L. Adams. Discontinuous finite element methods in thick diffusive problems. *Nucl. Sci. Eng.*, 137:298–333, 2001.
- [2] B. Ayuso and L. D. Marini. Discontinuous Galerkin methods for advection-diffusion-reaction problems. *SIAM J. Numer. Anal.*, 47(2): 1391–1420, 2009. ISSN 0036-1429.
- [3] I. Babuška and M. Suri. On locking and robustness in the finite element method. *SIAM J. Numer. Anal.*, 29(5):1261–1293, 1992. ISSN 0036-1429.
- [4] S. Chandrasekhar. *Radiative Transfer*. Oxford University Press, 1950.
- [5] R. Dautray and J.-L. Lions. *Mathematical Analysis and Numerical Methods for Science and Technology. Vol. 5. Evolution problems, I*. Springer-Verlag, Berlin, Germany, 1992. ISBN 3-540-50205-X; 3-540-66101-8.
- [6] A. Ern and J.-L. Guermond. Discontinuous Galerkin methods for

- Friedrichs' systems. I. General theory. *SIAM J. Numer. Anal.*, 44(2): 753–778, 2006. ISSN 0036-1429.
- [7] J.-L. Guermond and G. Kanschat. Asymptotic analysis of upwind discontinuous Galerkin approximation of the radiative transport equation in the diffusive limit. *SIAM J. Numer. Anal.*, 48(1):53–78, 2010. ISSN 0036-1429.
 - [8] E. W. Larsen. Deterministic transport methods. Technical Report LA-9533-PR, Los Alamos Scientific Laboratory, Los Alamos, NM,, 1982.
 - [9] E. W. Larsen. On numerical solutions of transport problems in the diffusion limit. *Nucl. Sci. Engr.*, 83:90–99, 1983.
 - [10] E. W. Larsen and J. B. Keller. Asymptotic solution of neutron transport problems for small mean free paths. *J. Mathematical Phys.*, 15:75–81, 1974. ISSN 0022-2488.
 - [11] E. W. Larsen and J. E. Morel. Asymptotic solutions of numerical transport problems in optically thick, diffusive regimes. II. *J. Comput. Phys.*, 83(1):212–236, 1989. ISSN 0021-9991.
 - [12] E. W. Larsen, J. E. Morel, and W. F. Miller, Jr. Asymptotic solutions of numerical transport problems in optically thick, diffusive regimes. *J. Comput. Phys.*, 69(2):283–324, 1987. ISSN 0021-9991.
 - [13] P. Lesaint and P.-A. Raviart. On a finite element method for solving the neutron transport equation. In *Mathematical Aspects of Finite Elements in Partial Differential Equations*, pages 89–123. Publication No. 33. Math. Res. Center, Univ. of Wisconsin-Madison, Academic Press, New York, 1974.
 - [14] F. Malvagi and G. C. Pomraning. Initial and boundary conditions for diffusive linear transport problems. *J. Math. Phys.*, 32(3):805–820, 1991. ISSN 0022-2488.
 - [15] J. C. Ragusa, J.-L. Guermond, and G. Kanschat. A robust S_N -DG approximation for radiation transport in optically thick and diffusive regimes. *J. Comput. Phys.*, 231(4):1947–1962, 2012. ISSN 0021-9991.
 - [16] W. Reed and T. Hill. Triangular mesh methods for the neutron transport equation. Technical Report LA-UR-73-479, Los Alamos Scientific Laboratory, Los Alamos, NM,, 1973.